NASA Technical Memorandum 100954
AIAA-88-2912

Internal Erosion Rates of a 10-kW Xenon Ion Thruster

Vincent K. Rawlin
Lewis Research Center
Cleveland, Ohio

Prepared for the
24th Joint Propulsion Conference
cosponsored by the AIAA, ASME, SAE, and ASEE
Boston, Massachusetts, July 11-13, 1988

NASA

AIAA'88

AIAA-88-2912
Internal Erosion Rates of a 10-kW Xenon Ion Thruster

Vincent K. Rawlin, NASA Lewis Research Center, Cleveland, OH

AIAA/ASME/SAE/ASEE 24th JOINT PROPULSION CONFERENCE

JULY 11-13, 1988/Boston, Massachusetts

INTERNAL EROSION RATES OF A 10-kW XENON ION THRUSTER

Vincent K. Rawlin
National Aeronautics and Space Administration
Lewis Research Center
Cleveland, Ohio 44135

SUMMARY

A 30 cm diameter divergent magnetic field ion thruster, developed for mercury operation at 2.7 kW, was modified and operated with xenon propellant at a power level of 10 kW for 567 hr to evaluate thruster performance and lifetime. The major differences between this thruster and its baseline configuration were elimination of the three mercury vaporizers, use of a main discharge cathode with a larger orifice, reduction in discharge baffle diameter, and use of an ion accelerating system with larger accelerator grid holes. At a xenon ion beam current of 5 A the engine produced a thrust of 0.33 N at a specific impulse of 4220 sec and an efficiency of 68 percent. There was no measurable screen grid erosion. However, grid thickness measurement uncertainties, combined with estimates of the effects of reactive residual facility background gases gave a minimum screen grid lifetime of 7000 hr. Discharge cathode orifice erosion rates were measured with three different cathodes with different initial orifice diameters. As the initial orifice diameter was increased from that of the baseline value, the erosion rate decreased to near zero.

Three potential problems were identified during the wear test. First, the upstream side of the discharge baffle eroded at an unacceptable rate, nearly two orders of magnitude greater than that of the baseline mercury thruster. Second, two of the main cathode tubes experienced oxidation, deformation, and failure after 227 and 243 hr of thruster operation. These failures are believed to be related to the cathode starting technique. Third, the accelerator grid impingement current was more than an order of magnitude higher than that of the baseline mercury thruster, implying a greater erosion rate. The impingement current increase is primarily due to a greater charge exchange ion current resulting from the higher beam current; operation at a higher neutral atom loss rate and; to a lesser extent, the higher facility pressure. The charge exchange ion erosion was not quantified in this test. There were no measurable changes in the accelerator grid thickness or the accelerator grid hole diameters.

INTRODUCTION

Inert gas ion thruster systems are being considered for primary propulsion for near-Earth, cislunar, and interplanetary missions (refs. 1 to 3). To reduce the specific mass and complexity of ion propulsion systems, it is desirable to increase the thrust produced by each thruster. This can be accomplished by increasing the ion beam current (propellant flow rate) and/or the beam voltage (propellant velocity). Increasing the beam voltage increases the thrust and specific impulse, but, it also reduces the ratio of output thrust to input power. Therefore, it is often desirable to increase the ion beam current as much as possible with minimal increases in the beam voltage. However, unless changes in other operating conditions can be made to offset the increased beam

E-4228

current with a given thruster there will be an increase in thruster internal erosion rates due to ion sputtering. Consequently, increased erosion rates may lead to thruster lifetimes which are insufficient for certain mission applications. Significant endurance test data exist for mercury ion thrusters with diameters between 5 and 30 cm (refs. 4 to 8) and power levels up to about 3 kW (ref. 8). Predictive analyses have been generated (refs. 9 to 11), but require information such as values of plasma potential and sputtering yield near threshold energies. The performance of 30 cm diameter xenon thrusters operating up to 7 kW has been reported in detail (refs. 12 and 13), but lifetests have only been conducted with low power (to 1.3 kW) xenon ion thrusters developed for north-south stationkeeping (refs. 14 and 15). Therefore, a test was conducted at NASA Lewis Research Center to identify and quantify the internal erosion rates of a 10 kW xenon ion thruster. This paper describes the results of that test.

APPARATUS

Thruster

Figure 1 is a schematic of a typical divergent field ion thruster showing the major components such as the main cathode, discharge baffle, and screen and accelerator electrodes. The thruster used for the wear test was a 30 cm diameter divergent magnetic field, mercury ion thruster built by Hughes Research Laboratories. This 3 kW mercury ion thruster design has been described in references 16 to 18, and is referred to here as the "baseline" thruster. This thruster had previously been operated with mercury for about 820 hr in endurance tests (thruster J2 in ref. 8). The thruster was modified, as described in reference 12, for use with xenon. Table I compares the geometries of the baseline mercury thruster and the modified thruster used for each segment of this test. The mercury propellant vaporizer-electrical isolator assemblies were removed, because they limited the xenon gas flow rates, and replaced with a 30 cm lengths of fluorocarbon elastomer tubing. In an attempt to simplify the thruster hardware and startup technique, none of the three main cathodes used heaters. All of the cathodes had 0.64 cm diameter tubes and 1.75 cm diameter radiation fins. Based on separate tests conducted in a bell jar, a cathode having a minimum orifice diameter of 1.47 mm was initially selected. For reasons discussed later baseline cathodes with initial orifice diameters of about 0.9 and 0.8 mm were used for test segments 2 and 3, respectively. The diameters of the multilayer baffles were reduced from 5.6 cm to 3.3 cm to achieve lower discharge voltage values as demonstrated in reference 12. The baseline set of ion optics was fabricated to flight prototype hardware specifications and, therefore, was not conducive to disassembly and inspection. Because of limitations on available hardware the baseline set was replaced with a set, identical to those on the 700 series thruster (ref. 7). This set had previously been tested over 5300 hr with mercury and xenon. The accelerator open area fraction was larger (0.43 instead of 0.24) which led to reduced discharge chamber performance because of increased neutral losses. For this test the molybdenum grids were attached to molybdenum perimeter rings which were held apart with aluminum oxide insulators. With this configuration the electrode spacing could be easily adjusted, and the entire assembly could be easily disassembled to measure grid thicknesses. The electrode spacing was about 1 mm at the center and 0.8 mm at the periphery of the active area.

Because of hardware availability, the neutralizer assembly was fabricated from laboratory components and was not optimized for xenon operation. The neutralizer cathode had a heater which was used during each startup sequence. The initial orifice diameter was 0.76 mm. Figure 2 shows the thruster mounted on a 1.2 m diameter vacuum flange.

Facility

The thruster was operated in a 0.9 m diameter port of a 7.6 m diameter by 21.3 m long vacuum chamber (fig. 3, tank 6). Fifteen 0.8 m diameter hydrocarbon oil diffusion pumps, with freon traps at about at about 236 K, were used to provide an initial, no load pressure of about 2×10^{-4} Pa (1.5×10^{-6} torr). The operational corrected pressure was about 1.9×10^{-3} Pa (1.4×10^{-5} torr) with a xenon gas flow rate of about 85 SCCM. Upon completion of testing the no load pressure had decreased linearly with time to approximately 1×10^{-4} Pa. Under gas load, the pressure gauge readings were corrected for xenon by dividing the indicated pressure by a factor of 2.8 as suggested in reference 19. A quadrupole residual gas analyzer was used to identify and estimate the partial pressure of facility background gases in the 1-100 AMU range, some of which could react with thruster internal components and alter erosion rates (ref. 20).

Power Supplies

Operation of the thruster utilized 60 Hz laboratory power supplies. The neutralizer cathode heater was powered with alternating current while the two keeper supplies had single phase, full wave rectified outputs. The open circuit voltage of the main cathode keeper supply was 800 V to facilitate cold cathode startups while the open circuit voltage of the neutralizer keeper supply was 350 V. The discharge supply consisted of an SCR controlled direct current output power supply connected in series with a transistorized series pass current regulator. This combination provided an open circuit voltage of about 80 V and a maximum limited current of 40 A. The positive and negative high voltage power supplies were motor driven, three phase, full wave bridge rectified units giving open circuit voltages of about 2500 V and overcurrent trip set points of about 8 A and 1 A, respectively. Both voltages were maintained constant to about ±30 V through the analog meter relays to close the loop on the primary power drive motors. Motor driven power supplies caused high voltage recycle times of approximately 7 sec. When an overcurrent was sensed on either supply, the primary power to both supplies was interrupted, both supply outputs were grounded, and the main discharge current was reduced from 31 A to about 9 A. The setting for the primary power of only the positive high voltage was reduced to about half of the run condition (taking about 3 sec); then the input power was restored and the grounding bars were lifted. A low value of beam current was extracted with voltages of +900 and -500 V. The positive high voltage was then increased to the 1800 V run value (taking another 3 sec) and then the discharge current was returned to its original value.

Propellant Feed and Control

High purity (99.995 percent pure), research grade xenon propellant from a single, 3000 liter bottle, was supplied to the main, cathode, and neutralizer

feed lines through flowmeters and control valves. The flowmeters operated by sensing the heat transferred between a heated capillary tube and the flowing gas and were factory calibrated for use with xenon. The gas flows could be adjusted in either an open-loop mode, with manual precision leak valves, or a closed-loop mode using piezoelectric leak valves controlled by comparing the flowmeter output signal and a reference signal. An optional gas purifier, which employed a heated titanium gettering element in a glass envelope, was connected in series with the gas bottle. However, the element was not heated for this test.

Data and Control Systems

Thruster discharge and extraction voltages and currents were measured with digital panel meters calibrated to be better than 1 percent in the range of interest. A multichannel datalogger was programmed to record eight critical thruster parameters as well as the three propellant flow rates and facility pressure. Each of the twelve channels were scanned sequentially for 2 sec and the data point average value printed every minute to allow observation of trends. Every 2 hr, each channel analog value was printed to allow weekend and off-shift data collection. For most of the test, the thruster and vacuum facility were operated in an unattended mode. In addition to the high voltage recycle logic discussed earlier, the thruster would be turned off if any of the following conditions persisted for more than about 1 min: discharge current below 5 A, a beam current below 4 A, or accelerator current greater than 0.06 A. Thruster and facility operation were also automatically terminated if the indicated facility pressure became greater than 5×10^{-2} Pa (4×10^{-4} torr).

PROCEDURE

Pretest

Prior to the extended test, critical thruster components were documented to allow comparisons with their post-test condition. Microphotographs of the cathodes were taken. Multilayer baffles were weighed, and the thicknesses measured. New screen mesh was used inside the cathode pole piece to catch and retain any sputtered baffle material. The ion optics were also inspected, disassembled, and individual grid thickness values were measured across two orthogonal diameters. Microphotographs were taken of both the extraction holes and accelerator grid charge exchange erosion (from prior use) after the electrodes were assembled.

Test Start

After each exposure to atmosphere, the thruster propellant feed lines were exposed to high vacuum for about 16 hr. For each discharge restart xenon flow rates of about 10 SCCM were established through the main and neutralizer cathodes. Power was applied to the neutralizer cathode heater to raise its temperature to about 1350 K for about 20 min. Open circuit voltages were then applied to both keeper (starting) electrodes and the discharge chamber anode. The neutralizer flow rate was then raised to 20 SCCM, the main propellant flow rate was set at about 32 SCCM, and the cathode flow rate was rapidly increased

to approximately 100 SCCM. A cold main cathode Paschen breakdown occurred in the thruster discharge chamber, and the main cathode and neutralizer keeper discharges and the main chamber discharges started simultaneously, due to the breakdown plasma. The cathode keeper, neutralizer keeper, and anode currents were 1, 2, and 9 A, respectively. The cathode flow was then rapidly reduced to 5 SCCM, and the neutralizer heater power reduced from 120 W (startup) to about 30 W (run power). The use of 30 W of neutralizer heater power maintained the neutralizer keeper discharge, in the absence of emission to the ion beam, with a xenon flow rate of 10 SCCM. The extraction voltages were then applied to obtain an ion beam.

At the beginning and end of the duration test, the discharge chamber performance and current carrying capability of the ion optics were measured as the propellant flow rate and thruster input power were increased to run conditions. After the main propellant flow rate was increased to approximately 72 SCCM, the extraction voltages were raised to +1800 and -500 V. Then the discharge current was increased to 36 A to give a discharge voltage of about 28 V and a beam current of 5 A. At this point, thruster control was put into an unattended operating mode as described earlier. Operation of the thruster at the nominal 10 kW input power operating point continued autonomously until a thruster shutdown occurred. When possible, thruster operation was resumed without any changes, otherwise the problem was corrected and the thruster was restarted.

Post Test

After each test segment, selected thruster components were weighed, measured and photographed to evaluate erosion. In addition, an attempt was made to quantify the effect of reactive facility gases on the xenon ion thruster component erosion rates. After the test had concluded, an analysis of the residual facility gases was conducted. It was found that about 50 percent of the total pressure was due to water vapor (probably from tank wall outgassing) and 25 percent due to nitrogen and oxygen from small air leaks. Based on the limitations of the residual gas analyzer, the balance of the residual gases was attributed to mercury (from prior testing) and long chain hydrocarbon pump oils. Water, oxygen, and nitrogen, all reactive species, were assumed to constitute three-fourths of the tank's no load pressure or 1.2×10^{-4} Pa (9×10^{-7} torr). Reference 10 has shown that water vapor and oxygen can affect the screen grid erosion rate in a manner similar to that of nitrogen. However, the magnitude of this effect with water vapor or oxygen has not been quantified. Therefore, it was assumed that water vapor and oxygen were as reactive as nitrogen. Thus, the mercury ion erosion rate - facility effect curves in figure 14 of reference 20 could be used to interpolate or extrapolate to erosion rate values expected in space by using erosion rate values experienced in this xenon thruster test.

RESULTS AND DISCUSSION

This section will discuss the events and results of a 567 hr test of a 30 cm diameter, divergent magnetic field xenon ion thruster operating at an input power of about 10 kW. First presented is a test chronology, followed by a review of high voltage recycle frequency, a thruster performance comparison between the start and end of the test, and finally a discussion of observed thruster component erosion.

Test Chronology

The wear test was started on June 23, 1987 and was terminated on August 12, 1987 for a duty cycle of approximately 50 percent. During the 567 hr of testing, the thruster was at full power for 89 percent of the time. Eleven percent of the time was spent at throttled conditions during scheduled performance mapping and restarts after 15 unscheduled thruster shutdowns.

Table II lists the test events as a function of run hour. The first shutdown (at run hour 4) was necessary to repair an electrical short between the accelerator grid harness wire and ground. The insulation failed when the accelerator grid power supply was accidentally driven to an output voltage of 2500 V (five times the normal value). Twelve "discharge out" shutdowns were due to an intermittently faulty optical isolation amplifier which caused the discharge current to be commanded to zero. The amplifier was replaced at run hours 115, 206, and 467 because, in each case, the shutdown frequency was increasing. The reason for amplifier failure is unknown. Two other shutdowns, at run hours 227 and 470, were more serious requiring replacement of the main discharge cathode. In both cases, the tantalum cathode tubes developed bulges and axial cracks just upstream of the 2.5 cm long cathode insert as shown in figure 4. These cracks, occurring within hours of restart after a "discharge out" shutdown, required increases in the cathode flow rate to maintain a discharge voltage of 28 V (described later). At run hour 542, it was noted that the neutralizer flow rate controller had malfunctioned during the previous 10 hr causing an abnormally low flow rate and high neutralizer keeper and coupling voltages. This malfunction caused severe neutralizer orifice sputtering damage rendering its operation unsatisfactory. Therefore, the neutralizer was turned off and grounded for the last 25 hr of the test with no other change in thruster operating conditions.

The last two shutdowns were anticipated. At run hour 559 the propellant supply was nearly exhausted causing the beam current to drop from 5 to 4 A and initiating a "low beam current" shutdown. The empty xenon bottle was replaced, the thruster was restarted, and 8 hr of post-test performance data were taken prior to removal and inspection of the thruster.

High Voltage Recycle Frequency

Figure 5 shows the cumulative number of high voltage recycles (recycles occurred when either the positive or negative high voltage power supply current limit was exceeded) and the recycle rate as functions of test time. Also indicated are the 17 thruster shutdowns. The recycle rate was initially about 10/hr for the first 30 hr and decreased to about 1/hr for the second 100 hr. After exposure to atmosphere to replace the original cathode, the recycle rate was very high but soon decreased to about 0.5/hr. After the second cathode replacement and exposure to air, the rate increased but only to about 1/hr for the last 100 hr. High voltage recycle rates of about 0.2/hr were typical during an endurance test of a similar 30 cm diameter thruster operated with mercury (ref. 7). The periods of very high recycle rate (greater than 4/hr), shown in figure 5, occurred after exposure to atmosphere (run hours 0 and 227) and some restarts after "discharge out" shutdowns (i.e., run hour 209).

Thruster Performance

Table III gives the measured thruster operating parameters for the baseline 3 kW mercury thruster and for the 10 kW xenon thruster from test segments 1, 2, and 3. Also shown are typical parameter variations for the xenon thruster. When comparing the xenon thruster values to those of the mercury thruster, it can be seen that the beam power was more than four times greater due to increases in operating voltage and current. The accelerator voltage was increased to prevent electrons from backstreaming from the neutralized beam through the larger accelerator grid holes. The accelerator impingement current was nearly 14 times greater than that of the baseline thruster because of the increased beam current, lower discharge chamber propellant efficiency, and to a lesser extent higher neutral atom density downstream of the grid due to the high facility pressure. The discharge voltage was lowered to reduce discharge chamber erosion, and the discharge current was increased to generate the desired ion current. For the first test segment, the cathode keeper voltage was similar to that with mercury. However, in test segments 2 and 3 (using J-series cathodes at high emission currents) the main cathode keeper voltage increased by a factor of 2. The unoptimized xenon neutralizer was operated at a flow rate 35 times greater than that of the baseline mercury neutralizer. The facility pressure (xenon thruster operating, corrected for xenon) was 25 times greater than that of the cryopumped mercury thruster facility. The increased pressure led to an ingested propellant flow rate which was added to the total thruster flow rate for propellant efficiency calculations as indicated in reference 12.

Thruster performance is primarily measured by the ability of the thruster to efficiently create ions in the discharge chamber and extract those ions with low total acceleration voltages. The discharge chamber efficiency is evaluated by measuring the discharge power required to produce 1 A of beam current as a function of the discharge propellant efficiency. Discharge chamber performance data taken at the start and end of the test are shown in figure 6 for a range of discharge chamber and cathode flow rates. These data are comparable to the decrease in discharge losses with increasing total flow rate discussed in reference 13. The apparent decrease in thruster performance with test time was believed to be a consequence of using smaller orificed cathodes for test segments 2 and 3; both of which required a greater cathode propellant flow rate to maintain the discharge voltage at the desired value of 28 V (see table III). Figure 7 shows the significant effect cathode flow rate can have on the propellant efficiency even at nearly constant values of discharge voltage. This trend has also been observed for mercury divergent field (ref. 21) and xenon ring cusp (ref. 22) thrusters. Comparing the curves at run hours 74 and 566, it was seen that the discharge propellant efficiency (about 0.89, at a discharge voltage of 28 V) was higher for the earlier data than it was (about 0.85) for the later data. This trend also existed at throttled conditions.

Table IV gives the calculated nominal thruster performance for the baseline mercury thruster and this modified J-series divergent magnetic field xenon thruster. The thrust reduction factors for beam divergence and multiply charged ions were previously measured for the mercury thruster and estimated, for this xenon thruster, using the technique indicated in reference 12. It was assumed that beam divergence losses could be minimized by proper grid design once an operating point was been selected. The losses due to multiply charged ions were estimated by assuming that this modified J-series xenon thruster had

the same doubly to singly charged ion current ratios as the 900 series thruster of reference 23 (see fig. 1 of ref. 12). The thrust loss factor due to multiply charged ions was then calculated. The thrust and power increased with xenon by factors of 2.5 and 3.8, respectively, due to the increased beam current and beam voltage. The specific impulse with xenon increased to 4220 sec because of the lighter atomic mass and the increased beam voltage. The reduction of specific impulse in test segments 2 and 3 resulted from a lower propellant efficiency with the small orificed cathodes. The thruster efficiency decreased from 75 to 68 percent primarily because of the inefficient neutralizer and lower discharge chamber propellant efficiency with the larger accelerator grid holes. If this thruster had been tested with J-series ion optics, an optimized neutralizer, and a more efficient ring-cusp magnetic field configuration, the thruster efficiency would be expected to increase to about 71 percent at a specific impulse of 4200 sec as predicted in reference 24.

Axial and radial components of the discharge chamber magnetic field were measured after the test and compared with values recorded in the Thruster Acceptance Test Log in 1976. There were no observed differences in magnetic field strength.

The current carrying capabilities of the ion accelerating system, measured at the beginning and end of the test, are shown in figure 8. At the end of the test, the beam current for a given total accelerating voltage was 30 percent greater than at the beginning. The reason for this increase is unknown but variations of this magnitude may be typical (ref. 12). The slopes for the two data sets were identical perhaps indicating a change in hot grid spacing or alignment. The data were found to approximately follow the expression $J_B = 1.7\ V_T^{1.8}$ where J_B is the beam current in amperes and V_T is the minimum total accelerating voltage in kilovolts. Over the range of interest (1 to 2.5 kV), this expression agrees within 20 percent with that for the baseline J-series optics given in reference 12. The perveance was expected to decrease by 60 percent due to the larger effective ion accelerating distance used here compared to that value used in reference 12 (1.91 mm versus 1.16 mm as defined in ref. 11). However, the perveance was also expected to increase due to the larger accelerator hole diameter. This increase was estimated to be either 40 or 110 percent depending on whether the experimental results of reference 25 or the analysis of reference 26 were used. The 5 A wear test operating point was conducted at a total voltage 500 V above the perveance limit value obtained from the expression given above.

Component Erosion Rates

To provide useful values of total impulse, ion thrusters must operate anywhere from a few thousand to more than 20 000 hr depending on the mission. However, not all of the ions created in an ion thruster provide thrust. The ions that do not provide thrust impinge on various surfaces with a wide range of energies and densities and slowly erode those surfaces by a process called sputtering. At low ion energies (about 30 eV) sputter yields for xenon ions on refractory metals are about 10^{-4} atoms per ion, while 2300 eV ions produce nearly three atoms per ion. Reference 20 has described how the internal erosion rates of ion thruster components can be reduced by facility effects yielding incorrect lifetimes. This effect occurs if the arrival rate of certain facility gases, which become reactive in the discharge chamber, are significant

when compared to the removal rate of the surface material. This section describes component erosion and other wearout mechanisms observed during this test.

Discharge cathode. - A major concern for discharge hollow cathodes used in ion thrusters is erosion of the orifice plate due to ion bombardment. Based on earlier work performed with mercury propellant (refs. 11 and 27 to 29) and unpublished work with xenon, the initial cathode selected for this test at high emission current had an orifice diameter of 1.47 mm. This diameter is larger than the baseline thruster cathode orifice of 0.76 mm because the emission current was 2.6 times higher. The large orifice cathode had previously been characterized for 38 hr in separate cathode tests at emission currents up to 60 A with no measured dimensional changes. At run hour 227 of this test (with an emission current of 31 A), the cathode tube cracked and the test was interrupted. Inspection of the cathode revealed no change in orifice dimensions within the uncertainty of the measurement ($\pm 1.3 \times 10^{-5}$ cm). However, a 1 cm long portion of the tantalum tubing was found to be bulging (fig. 4), beginning at a point 2.7 cm upstream from the cathode orifice plate and cracked axially allowing loss of cathode propellant. Spectroscopic analysis of the tubing showed that the inside surface had been oxidized. At the beginning of the test, the glass envelope of the gas purifier that was being used was found to be broken, possibly allowing air to mix with the high purity xenon which was supplied to the cathode. After replacing the glass envelope, the cathode discharge was restarted and normal thruster operation was achieved.

After 243 additional hours of testing, the second cathode failed in a manner identical to the first cathode for an unknown reason. When no air leak could be found, the operating technique was examined. Both failed cathodes had been tested in a diode configuration and exposed to atmosphere several times before being used in an ion thruster. In all tests, the main discharge cathodes were started without using a heater and brought to temperature during use by ion bombardment self-heating. It is postulated that during use, some of the barium oxide evaporates from the hot insert and deposits on the upstream portions of the tantalum tube. When exposed to air, this barium oxide may absorb water to form barium hydroxide which could later decompose and react with the warm tantalum tube of the operating cathode. The brittle inner surface could then expand at a different rate than the ductile outer surface leading to stresses and cracked tubing. Based on this postulate, an obvious solution would be to heat the cathode and insert before the discharge was started as was previously done with mercury thrusters. Hollow cathodes tested with mercury have accumulated more than 100 000 hr of operating time in ground and space tests without observing a failure of this type. In all of those tests, heaters were used to activate the insert and avoid mercury condensation. Additional support for the use of cathode heaters is provided by the fact that the neutralizer cathode accumulated more than 1000 hr of operation in this test on xenon without degradation of the tantalum tubing. The neutralizer discharge was started more than 30 times, always with the use of a heater. This procedure was also used in the successful 4300 hr test of a 25 cm diameter xenon ion thruster (ref. 14).

Because the original discharge cathode experienced no measurable changes in orifice dimensions, the second and third cathodes used were of the J-series geometry (table I) to quantify the erosion rates with orifices smaller in diameter than 1.47 mm. As mentioned earlier, the second cathode had also been

previously tested in a nonthruster configuration at emission current values to 90 A. In those tests, the orifice diameter increased to 0.90 mm, the value at the beginning of test segment 2. When inspected at run hour 470, the orifice diameter had increased to 0.96 mm. The third cathode, installed at run hour 470 was unused and had an initial minimum diameter of 0.79 mm. After 97 hr of testing, the cathode orifice diameter had increased to 0.90 mm. A criterion given in reference 11 states that excessive erosion of the hollow cathode orifice would occur if the ratio of emission current to orifice diameter exceeds 12 A/mm. This criterion was based on data from reports where the orifice diameters were less than 1 mm and the emission current was 15 A or less. Figure 9 shows the orifice diameter erosion rate as a function of the ratio of emission current to orifice diameter taken from reference 11. Also shown are the cathode erosion rates for the three 10 kW xenon test segments. For a given emission current, the erosion rate drops rapidly as the orifice diameter is increased. Cathodes with 0.76 mm diameter and larger orifice diameters have been operated at various emission currents and propellant types with no measurable erosion and are listed in table V and shown in figure 9. Based on these data, the original criterion of reference 11 appears to be conservative.

Neutralizer Cathode

Because laboratory hardware unoptimized for xenon was used, little emphasis was placed on neutralizer performance or lifetime. The neutralizer cathode orifice diameter was documented at the start of the test. No dimensional changes were observed at run hours 227 and 470. At run hour 532, the neutralizer expellant flow controller failed and reduced the flow to near zero. The neutralizer keeper voltage had risen to about 80 V for 10 hr in this "starved" condition. Normal operation could not be restored, even with increased flow rate through the manual control valve. Therefore, the neutralizer system was turned off and grounded for the last 25 hr of the test and neutralizing electrons were obtained from the facility walls. Upon inspection, it was found that the neutralizer cathode orifice had rapidly eroded to a diameter of 2.8 mm. Severe neutralizer cathode orifice erosion has been experienced before under similar low flow conditions (ref. 5 and 27).

Discharge Baffles

To improve the ionization efficiency of divergent magnetic field ion thrusters, a metallic disc or baffle is placed downstream of the hollow cathode. Thruster performance is improved, but both sides of the baffle are bombarded by ions. For this test the baffle consisted of separate upstream and downstream surfaces which could be weighed independently. For the first 227 hr of the test, two iron baffles were used. The baffles were inspected when the test was interrupted to replace the first cathode. The weight loss rate of the downstream baffle was 0.26 mg/hr and the erosion was uniform over the entire surface, giving a rate of change in baffle thickness of 39 μm/khr. Correcting this erosion rate for the facility effect yields an erosion rate, anticipated for space, of about 45 μm/khr. This rate is about 2.1 times greater than that of the 3 kW mercury thruster (ref. 30). While this component can be made thick enough to have sufficient lifetime, the quantity of eroded material and subsequent deposition rate may be intolerable.

The upstream surface had a weight loss rate of 0.61 mg/hr. This erosion was not uniform over the smaller area exposed by the baffle mounting flange. Thickness measurements before and after this test segment gave erosion profiles as shown in figure 10. The initial erosion had accumulated from previous testing with widely varying conditions. The maximum rate of change in baffle thickness at constant thruster conditions for this segment of the test was about 660 μm/khr. This is 66 times greater than that experienced in the 3 kW, J-series mercury ion thruster endurance tests (refs. 8 and 30). The effects of background facility gases were probably negligible at this high erosion rate. The wear mechanism appears to be sputtering from the cathode discharge, although the details leading to such a high erosion rate are not understood at this time.

New baffles were used for the second test segment with the intention of using tantalum covers over the mild steel magnetic baffle as is done in the mercury thruster. Unintentionally, the mild steel disc was installed as the downstream surface and the two tantalum pieces were placed upstream of it. The baffles were undisturbed for the last two test segments which both used J-series geometry cathodes. The weight loss rate for the downstream mild steel baffle was 0.077 mg/hr and again the erosion was uniform. This erosion gave a measured rate of change of baffle thickness of only 12 μm/khr, about three times less than the first test segment. The erosion rate, corrected for facility effects was about 25 μm/khr. The reason for the different erosion rates is unknown, but may be related to the different cathode orifice diameters. With the smaller cathode orifice diameters (segments 2 and 3) the cathode keeper voltage was higher than for segment 1, and it was more difficult to obtain a 5 A beam current at a discharge voltage of 28 V. For the tantalum baffle facing the cathode, the weight loss rate was high (1.2 mg/hr) about double that observed in test segment 1. Micrometer thickness measurements again showed a very peaked erosion pattern over the exposed 2 cm diameter area with a maximum rate of change in thickness of about 900 μm/khr or 90 times that of the 3 kW mercury thruster. A redesign of the cathode pole piece-baffle assembly is required. An attractive alternative to the divergent field thruster with a baffle is the ring cusp magnetic field discharge chamber which has no baffle to erode. This geometry has also demonstrated more efficient discharge chamber operation (refs. 13 and 14). A ring cusp configuration has also undergone extensive testing with xenon at low power levels (about 1.3 kW) for more than 4300 hr (ref. 14) and has been performance tested (refs. 32 to 34) with xenon at power levels up to 7.3 kW (ref. 13). Because the very high erosion rates of the upstream side of the baffle were unacceptable, the deposition rates of sputtered material on the screen mesh inside the cathode piece were not analyzed.

Screen Grid

The screen grid of the ion accelerating system is at cathode potential. Ions which are not extracted into the beam fall from discharge plasma potential (near anode voltage) to cause sputter damage. The resulting erosion rate, along with the finite screen grid thickness, determines the grid lifetime. The screen grid was the life limiting component of the 3 kW mercury ion thruster (ref. 7). In selecting the operating point of the 10 kW xenon thruster, consideration was given to screen grid lifetime. Because increases in screen grid thickness degrade ion accelerator system current extraction capabilities, solutions to maintaining long grid life at higher thruster power were sought in discharge chamber operation. Acceptable screen grid erosion rates (6.4 to

12 μm/khr) were obtained in extended testing of the J-series, 2 A mercury thruster operating with a discharge voltage of 32 V refs. 8 and 20). The goal for this test with a xenon ion beam current of 5 A was to maintain a similar lifetime. To offset the expected increased erosion due to increased current density and higher sputter yields with xenon (ref. 12), the discharge voltage was lowered to 28 V. The grid thickness was measured before and after 567 hr of testing, with an electronic micrometer. Within a ±2.5 μm thickness uncertainty, there was no measurable erosion. Figures 11(a) and (b) show photomicrographs of the central portion of the upstream side of the screen grid before and after this test. When viewed at higher magnifications, the sharp edges of the holes on the upstream surface have been smoothed from discharge ion bombardment (fig. 11c). The triangular area between any three adjacent holes appears to be unworn and possibly a net deposition site. The downstream side of the grid (fig. 11(d)) appeared unworn. There was a discoloration due to a thin film deposit, out to a radius of 10 cm, at the triangular region between any three holes. A possible source of these deposits will be discussed later.

An estimate of the worst case screen grid erosion rate was made based on measurement uncertainties, and the facility effect described earlier. The ±2.5 μm thickness measurement uncertainty could lead to an erosion rate of 9 μm/khr. Due to the facility effect this rate could possibly be as high as 27 μm/khr. The screen grid has a beginning-of-life thickness of 380 μm which should permit at least 7000 hr of operation before it wears to half thickness. Operation with a 190 μm thick screen grid has been demonstrated (ref. 7). As shown in reference 20, when a small amount of nitrogen was introduced into the discharge chamber, the spectroscopic signal intensity from erosion of the molybdenum screen grid was significantly reduced. The addition of nitrogen to the thruster propellant could possibly extend the 7000 hr minimum screen grid lifetime by a factor of 2 or 3.

Accelerator Grid

The accelerator grid was about 500 V negative of the neutralized beam plasma and about 2300 V negative of the discharge chamber potential. A small fraction (about 1 percent) of the ions which are extracted from the discharge chamber cause an accelerator grid impingement current. This current consists of two components: (1) direct impingement by high angle, high energy beam ions and (2) charge exchange ions formed in the interelectrode space, acceleration grid hole, or downstream of the accelerator grid. Those charge exchange ions formed in the acceleration region leave the thruster with a wide range of dispersion angles. Those charge exchange ions formed in the deceleration region are focused onto the downstream surface of the accelerator grid to create erosion pits and grooves like those shown in figure 12(a). The grids used in this test had been previously tested for over 5300 hr on mercury and xenon thrusters. Figure 12(a) shows the central portion of the downstream side of the accelerator grid at the start of this test. Deep charge exchange pits and grooves were apparent. The rough surface around each hole is the region of little erosion. The blurry hexagonal pattern around each hole is a deep groove connecting the charge exchange pits. The dark spot at the center of each pit is believed to be a small hole eroded completely through the accelerator grid. Similar photographs were taken at different radii, and the charge exchange holes appear to end at a radius between 5 and 7.6 cm. When this grid set was used on mercury thrusters in a cryopumped facility, the accelerator impingement current was

typically 0.25 percent of the beam current (ref. 35). Throughout this test with xenon, the accelerator current was about 0.94 percent of the beam current. The local ratio of accelerator impingement current to ion beam current is equal to the product of the local neutral density, the charge exchange cross section, and a charge exchange volume. Analyses to calculate an absolute value of accelerator impingement current are complex (refs. 11, 36, and 37) and were beyond the scope of this paper. However, a relative comparison was made for a hypothetical thruster operating either with mercury at a 2 A beam current or with xenon at a 5 A beam current (ref. 38). Values for the facility pressure were assumed to be 1.3×10^{-4} Pa (1×10^{-6} torr) for the mercury thruster and 1.9×10^{-3} Pa (1.4×10^{-5} torr) for the xenon thruster. A value of 6×10^{-19} m^2 was used for the charge exchange cross sections of mercury and xenon (refs. 11 and 39). The charge exchange volume was assumed to be equal to the product of the screen grid open area and a constant 2 cm length. For a fixed propellant efficiency (0.9 assumed) and neutral gas temperature, the ratio of accelerator charge exchange current to beam current varies directly with beam current and, inversely, with the square root of the propellant atomic mass. For this case, a charge exchange current to beam current ratio increase of 3.7 times was calculated. The contributions of the facility neutral atoms to the charge exchange current ratios were estimated to be 3 and 20 percent for the mercury and xenon thrusters, respectively. The calculated relative value of 3.7 is comparable to the observed value of 3.8 (total accelerator current to beam current ratio).

At the end of the test, photographs were taken with the grids disassembled. Figure 12(b) shows that the charge exchange erosion holes are larger than those in figure 12(a) and are triangular in shape. In addition, the radius to which the holes extend has increased to 10 cm. Figure 12(c) shows the upstream side of the accelerator grid at the thruster axis. The charge exchange holes are chamfered. It is postulated that this wear was due to charge exchange ions that went through the hole, were repelled by the positive potential of the screen grid, and were then accelerated back to the upstream surface of the accelerator grid. It is possible that some of this sputtered material resulted in the deposits on the downstream surface of the screen grid. These deposits may have loosened after exposure to air or thermal cycling and contributed to the increased high voltage recycle rate. Erosion rates due to charge exchange ions were not quantified, but appear to be significant with light gases, higher values of beam current, and higher accelerator grid potential. The use of a smaller hole accelerator grid could appreciably reduce the charge exchange ion current by reducing the neutral density from the thruster. The use of small hole accelerator grids would also permit the use of lower values of grid potential to avoid electron backstreaming effects. If the grid potential had been 300 instead of 500 V, the amount of material eroded would have been expected to be decreased by a factor of 2. The use of three-grid optics (with a decelerator grid at near ground potential) has been shown (ref. 40) to reduce the percentage of accelerator impingement current by 26 percent. Further testing, with lower thruster neutral losses and lower facility pressures, is required to quantify the potential problem of excessive charge exchange ion erosion of the accelerator grid. There were no measurable changes in accelerator grid thickness or accelerator grid hole diameters.

CONCLUSIONS

This test was the first extended operation of a high power xenon ion thruster. The 30 cm diameter divergent magnetic field thruster tested was originally designed for 2.7 kW, 2 A beam current operation with mercury. It was modified and operated on xenon propellant for 567 hr at an input power of 10 kW and a beam current of 5 A. The thrust produced was 0.33 N at a specific impulse of 4220 sec and a thruster efficiency of 68 percent.

The primary wear mechanisms were expected to be low energy ion sputtering of the cathode orifice and the screen grid. Therefore, a cathode having a larger orifice diameter than that of the original mercury thruster was used. In addition, the discharge voltage was lowered to offset the expected increase in screen grid erosion due to the higher value of beam current and higher sputter yield of xenon compared to mercury. The results showed no enlargement of the cathode orifice after 227 hr or reduction of the screen grid thickness after 567 hr. Estimated uncertainties in the grid thickness measurement and the effects of reactive residual facility background gases give a minimum screen grid lifetime of 7000 hr (to wear to half thickness).

Three other wearout modes were identified. The upstream side of the baffle eroded nonuniformly, giving maximum rates of thickness change nearly two orders of magnitude greater than those of the baseline mercury thruster. These rates are unacceptable and will require a significant design change. One potential solution to the problem is to use the ring cusp magnetic geometry which does not employ a baffle. The second problem observed was that of oxidation, deformation, and cracking of the tantalum cathode tube probably brought about by the cold cathode startup technique. The third potential problem is accelerator grid wearout due to charge exchange ion erosion. The accelerator grid impingement current increased, as expected, with the lighter xenon gas and higher beam current; however, the erosion rate was not measured. About 80 percent of the charge exchange ion current in this test was estimated to be due to the thruster operating conditions with the balance due to the high facility pressure.

It is recommended that a parametric program be conducted to fully understand the impact of facility effects on all facets of high power inert gas ion thruster lifetime to avoid and/or minimize the necessity of long term tests in cryogenically pumped facilities.

REFERENCES

1. Sponable, J.M., and Penn, J.P., "An Electric Orbital Transfer Vehicle for Delivery of NAVSTAR Satellites," AIAA Paper 87-0985, May 1987.

2. Aston, G., "Ferry to the Moon," Aerospace America, Vol. 25, No. 6, June 1987, pp. 30-32.

3. Galecki, D.L., and Patterson, M.J., "Nuclear Powered Mars Cargo Transport Mission Utilizing Advanced Ion Propulsion," AIAA Paper 87-1903, June 1987. (NASA TM-100109.)

4. Nakanishi, S., and Finke, R.C., "A 9700-Hour Durability Test of a 5-cm Diameter Ion Thruster," AIAA Paper No. 73-1111, Oct. 1973. (NASA TM X-68284.)

5. Dulgeroff, C.R., Beattie, J.R., Poeschel, R.L., and Hyman, J., Jr., "Ion Thruster System (8-cm) Cyclic Endurance Test," NASA CR-174745, 1984.

6. Kerslake, W.R., "SERT II Thrusters - Still Ticking After Eleven Years," AIAA Paper 81-1539, July 1981. (NASA TM-81744.)

7. Collett, C., "Thruster Endurance Test," NASA CR-135011, 1976.

8. Bechtel, R.T., Trump, G.E., and James, E.J., "Results of the Mission Profile Life Test," AIAA Paper 82-1905, Nov. 1982.

9. Mantenieks, M.A., and Rawlin, V.K., "Sputtering in Mercury Ion Thrusters," AIAA Paper 79-2061, Oct. 1979. (NASA TM-79266.)

10. Beattie, J.R., "A Model for Predicting the Wearout Lifetime of the LeRC/Hughes 30 cm Mercury Ion Thruster," AIAA Paper 79-2079, Oct. 1979.

11. Kaufman, H.R., "Technology of Electron-Bombardment Ion Thrusters," Advances in Electronics and Electron Physics, Vol. 36, L. Marton, ed., Academic Press, Inc., New York, 1974, pp. 265-373.

12. Rawlin, V.K., "Operation of the J-Series Thruster Using Inert Gas," AIAA Paper 82-1929, Nov. 1982.

13. Patterson, M.J., "Performance Characteristics of Ring Cusp Thrusters with Xenon Propellant," AIAA Paper 86-1392, June 1986. (NASA TM-87338.)

14. Beattie, J.R., Matossian, J.N., and Robson, R.R., "Status of Xenon Ion Propulsion Technology," AIAA Paper 87-1003, May 1987.

15. Shimada, S., Sato, K., Takegahara, H., and Kajiwara, K., "20 mN Class Xenon Ion Thruster for ETS-VI," AIAA Paper 87-1029, May 1987.

16. "The 30 cm Ion Thrust Subsystem Design Manual," NASA TM-79191, 1979.

17. Schnelker, D.E., Collett, C.R., Kami, S., and Poeschel, R.L., "Characteristics of the NASA/Hughes J-Series 30 cm Engineering Model Thruster," AIAA Paper 79-2077, Oct. 1979.

18. Bechtel, R.T., "The 30 cm J-Series Mercury Bombardment Thruster," AIAA Paper 81-0714, Apr. 1981.

19. Holanda, R., "Sensitivity of Hot-Cathode Ionization Vacuum Gages in Several Gases," NASA TN D-6815, 1972.

20. Rawlin, V.K., and Mantenieks, M.A., "Effect of Facility Background Gases on Internal Erosion of the 30 cm Hg Ion Thruster," AIAA Paper 78-665, Apr. 1978. (NASA TM-73803.)

21. Rawlin, V.K., "Performance of 30-cm Ion Thrusters with Dished Accelerator Grids," AIAA Paper 73-1053, Oct. 1973. (NASA TM X-68294.)

22. Beattie, J.R., Matossian, J.N., Poeschel, R.L., Rogers, W.P., and Martinelli, R., "Xenon Ion Propulsion Subsystem," AIAA Paper 85-2012, Sept. 1985.

23. Poeschel, R.L., "The 2.5 kW Advanced Technology Ion Thruster," NASA CR-135076, 1976.

24. Rawlin, V.K., and Patterson, M.J., "High Power Ion Thruster Performance," NASA TM-100127, 1987.

25. Rawlin, V.K. "Sensitivity of 30 cm Mercury Bombardment Ion Thruster Characteristics to Accelerator Grid Design," AIAA Paper 78-668, Apr. 1978. (NASA TM-78861.)

26. Poeschel, R.L., "High Power and 2.5 kW Advanced Technology Ion Thrusters," NASA CR-135163, 1977.

27. Rawlin, V.K., and Kerslake, W.R., "Durability of the SERT II Hollow Cathode and Future Applications of Hollow Cathodes," AIAA Paper 69-304, Mar. 1969.

28. Mirtich, M.J., "Investigation of Hollow Cathode Performance for 30-cm Thrusters," AIAA Paper 73-1138, Oct. 1973. (NASA TM X-68298.)

29. Beattie, J.R., "Extended Performance Technology Study: 30-cm Thruster," NASA CR-168259, 1983.

30. James, E.L., and Bechtel, R.T., "Results of the Mission Profile Life Test First Test Segment: Thruster J1," AIAA Paper 81-0716, Apr. 1981.

31. Sovey, J.S., "A 30-cm Diameter Argon Ion Source," AIAA Paper 76-1017, Nov. 1976. (NASA TM X-73509.)

32. Sovey, J.S., "Improved Ion Containment Using a Ring-Cusp Ion Thruster," Journal of Spacecraft and Rockets, Vol. 21, No. 5, Sept.-Oct. 1983, pp. 488-495.

33. Poeschel, R.L., "Development of Advanced Inert-Gas Ion Thrusters," NASA CR-168206, 1983.

34. James, E.L., "Advanced Inert Gas Ion Thrusters," FR-R83-05-39, Loral Electro-Optical Systems, Pasadena, CA, July 1984, NASA CR-168192.

35. Rawlin, V. K., "Studies of Dished Accelerator Grids for 30-cm Ion Thrusters," AIAA Paper 73-1086, Oct. 1973. (NASA TM X-71420).

36. Kerslake, W.R., "Charge-Exchange Effects on the Accelerator Impingement of an Electron-Bombardment Ion Rocket," NASA TN D-1657, 1963.

37. Staggs, J.F., Gula, W.P., and Kerslake, W.R., "Distribution of Neutral Atoms and Charge-Exchange Ions Downstream of an Ion Thruster," Journal of Spacecraft and Rockets, Vol. 5, No. 2, Feb. 1968, pp. 159-164.

38. Wilbur, P.J., Private Communication.

39. Smirnov, B.M., and Chibisov, M.I., "Resonance Charge Transfer in Inert Gases," Soviet Physics - Technical Physics, Vol. 10, No. 1, July 1965, pp. 88-92.

40. Rawlin, V.K., and Hawkins, C.E., "Increased Capabilities of the 30-cm Diameter Hg Ion Thruster," AIAA Paper 79-0910, May 1979. (NASA TM-79142.)

TABLE I. - J-SERIES/WEAR TEST HARDWARE

Thruster	Propellant feed and electrical isolator	Main cathode		Discharge baffles		Ion optics						Cold grid-to-grid spacing, mm
		J-Series hardware	Minimum initial orifice diameter, mm	Material		Screen			Accelerator			
				Upstream surface	Downstream surface	Diameter, cm	Hole diameter, mm	Open area fraction	Hole diameter, mm	Thickness, mm	Open area fraction	
Baseline 2.7 kW mercury, J-series	Mercury vaporizer-isolator assemblies	Yes	0.76	Tantalum cover	Tantalum cover	5.3	1.91	0.67	1.14	0.38	0.24	0.5
High power 10 kW xenon Test segment												
1	Fluoro-carbon elastomer tubing	No	1.47	Iron	Iron	3.3	1.91	0.67	1.52	0.51	0.43	1.0
2		Yes	.90	Tantalum	Iron	3.3	1.91	.67	1.52	.51	.43	1.0
3		Yes	.79	Tantalum	Iron	3.3	1.91	.67	1.52	.51	.43	1.0

TABLE II. - 10 kW XENON THRUSTER WEAR TEST CHRONOLOGY

Test segmemt	Run hour	Event/Shutdown	Comment
1	0	Test start	6-23-87
	4	Wire insulation failure	
	12	Discharge out	Reason unknown
	60	Discharge out	
	67	Discharge out	
	73	Discharge out	
	102	Discharge out	
	115	Discharge out	Replace isolation amplifier
	198	Discharge out	
	206	Discharge out	Replace isolation amplifier
	227	High discharge voltage	Main cathode tube cracked Replace main cathode and discharge baffles
2	227	Test restart	
	398	Discharge out	
	437	Discharge out	
	467	Discharge out	Replaced isolation amplifier
	470	High discharge voltage	Main cathode tube cracked Replace main cathode
3	470	Test restart	
	559	Low beam current	Xenon bottle empty
	567	End of test	Inspect thruster, 8-12-87

TABLE III. - MEASURED THRUSTER PARAMETERS

Parameter	3 kW mercury (acceptance test data)	Nominal 10 kW xenon		Typical variation
		Test segment 1	Test segment 2, 3	
Screen voltage, V	1100	1800	1800	±30
Beam current, A	2.0	5.0	5.0	0.1
Accelerator voltage, V	308	510	510	30
Accelerator current, A	0.0033	0.048	0.046	0.002
Discharge voltage, V	32	28	28	0.5
Anode current, A	14	36	36	1.0
Cathode keeper voltage, V	4	4.5	8.7	1.0
Cathode keeper current, A	1.0	1.0	1.0	0.05
Neutralizer keeper voltage, V	13	14	14	1.0
Neutralizer keeper current, A	1.8	2.5	2.5	0.05
Neutralizer common floating voltage, V	9	16	16	1.0
Facility pressure, Pa (torr)	8.6×10^{-5} (6.5×10^{-7})	2.1×10^{-3} (1.6×10^{-5})	1.7×10^{-3} (1.3×10^{-5})	0.4^{-3} (0.3^{-5})
Main flow rate, eq A	1.99	4.80	5.14	0.3
Cathode flow rate, eq A	0.06	0.21	0.26	0.1
Neutralizer flow rate, eq A	0.02	0.70	0.70	0.03
Ingested flow rate, eq A	———	0.18	0.15	0.03

TABLE IV. - NOMINAL THRUSTER PERFORMANCE

Parameter	3 kW mercury (acceptance test data)	10 kW xenon	
		Test segment 1	Test segment 2, 3
Thrust reduction factor due to beam divergence	0.99	[a]0.98	[a]0.98
Thrust reduction factor due to multiply charged ions	0.98	[a]0.96	[a]0.97
Thrust, N	0.13	0.33	0.33
Specific impulse, sec	3090	4220	4020
Input power, kW	2.64	10	10
Efficiency	0.75	0.68	0.65

[a]Estimated from reference 12.

TABLE V. - MAIN CATHODES WITH NO MEASURABLE EROSION

Reference	Minimum orifice diameter, mm	Emission current, A	Propellant type
30	0.76	12	Mercury
29	1.27	40	Mercury
31	1.5	25	Argon
10-kW wear test	1.47	31	Xenon

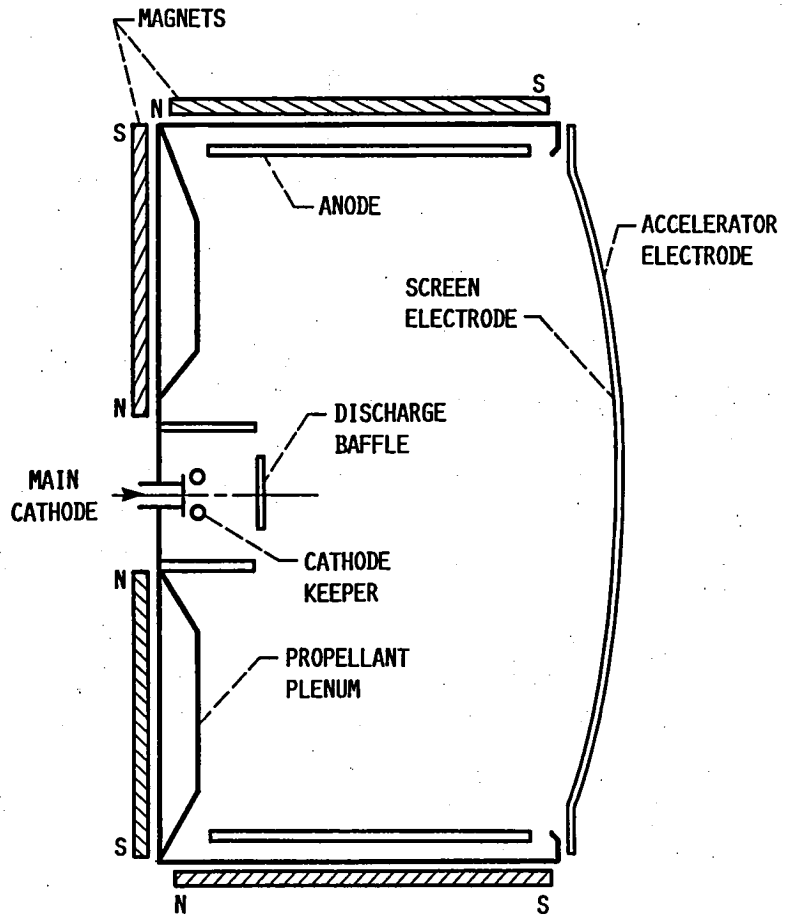

FIGURE 1. - SECTION VIEW OF DIVERGENT MAGNETIC FIELD THRUSTER.

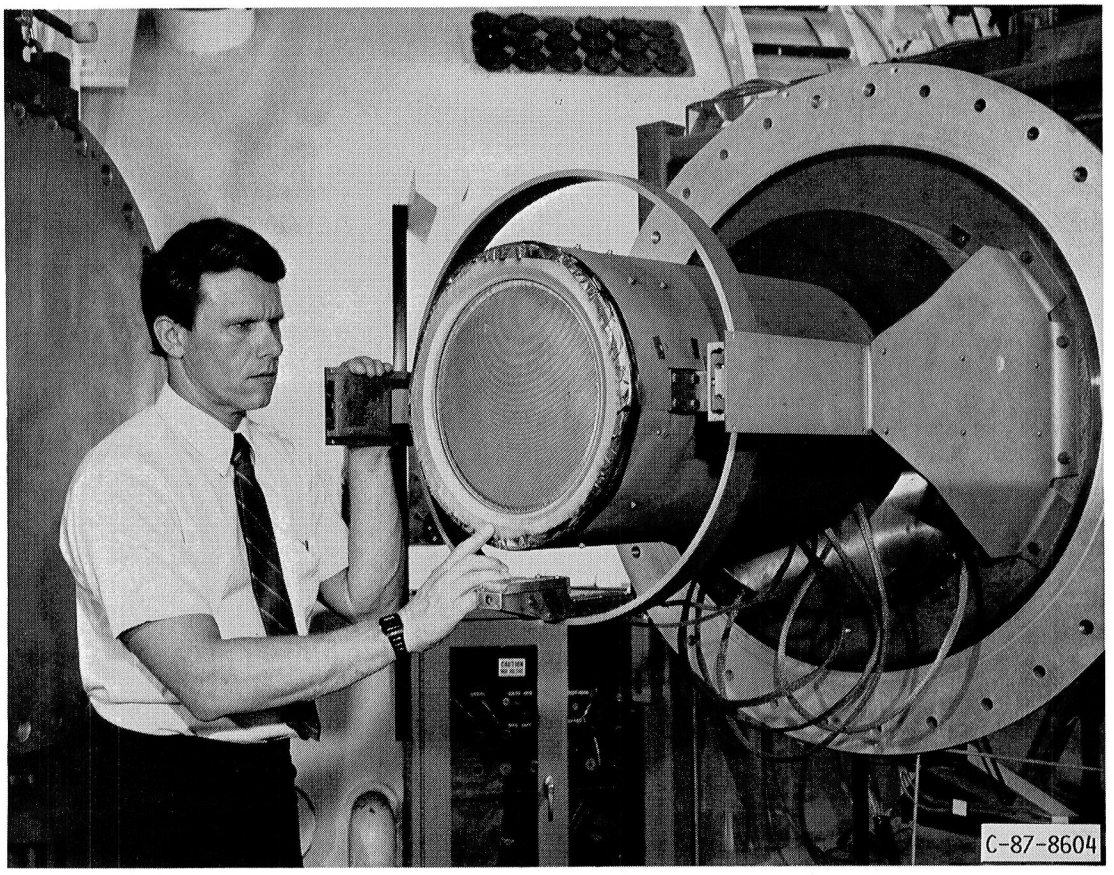

FIGURE 2. - 10 kW XENON THRUSTER.

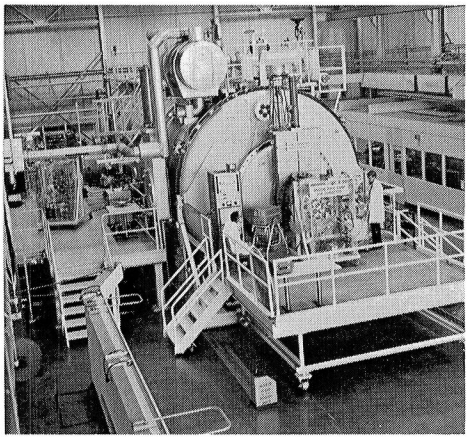

TANK 5

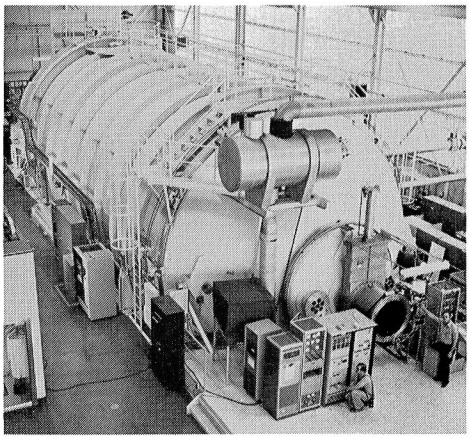

TANK 6

FIGURE 3. - 10 kW XENON THRUSTER TEST FACILITY, 7.6 mm DIAM x 21.3 m LONG.

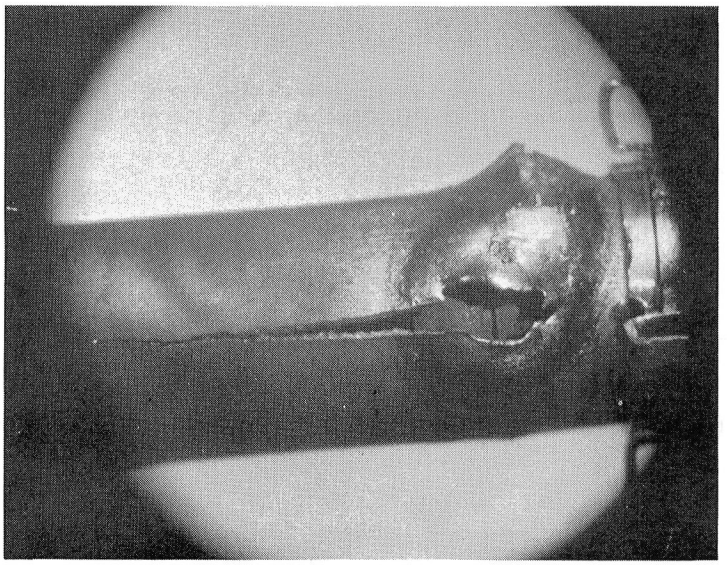

FIGURE 4. - DEFORMATION AND CRACK IN MAIN CATHODE TUBE, 2.7 cm UPSTREAM OF THE ORIFICE PLATE.

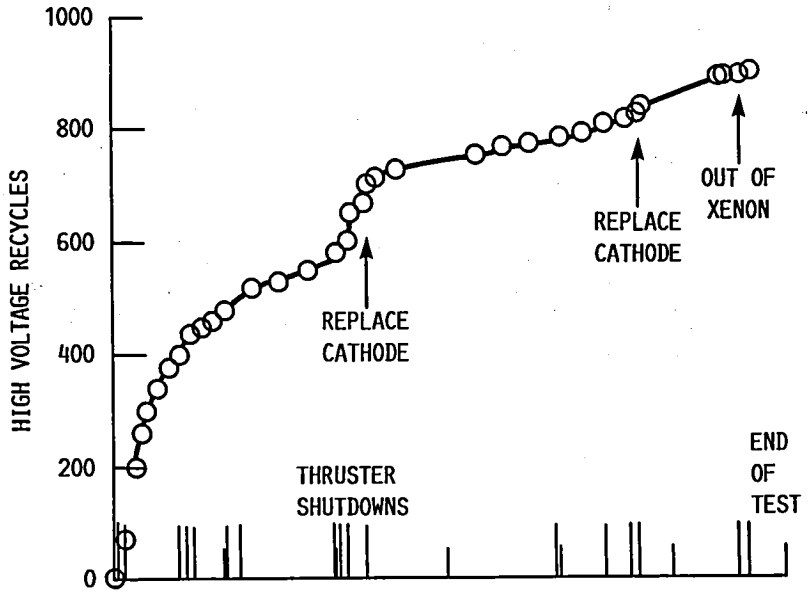

(a) HIGH VOLTAGE RECYCLES.

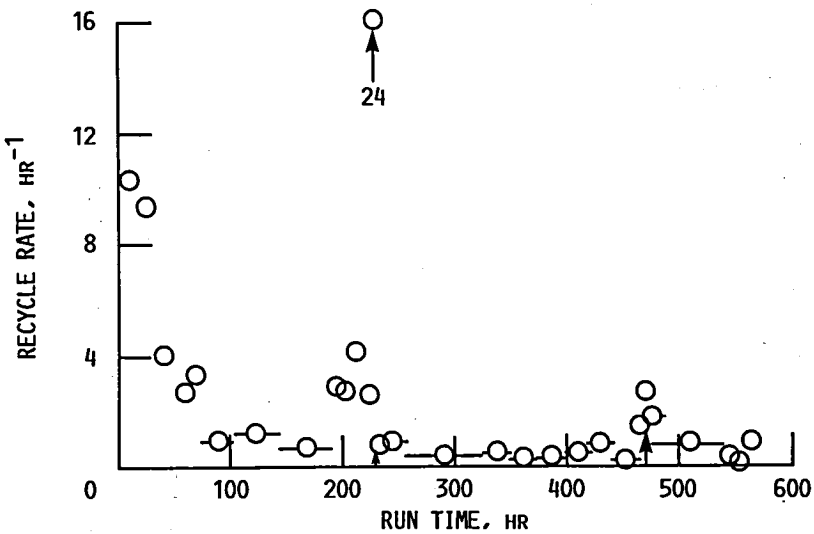

(b) RECYCLE RATE, HR^{-1}

FIGURE 5. - FREQUENCY AND TOTAL NUMBER OF HIGH VOLTAGE RECYCLES AS FUNCTIONS OF TEST TIME.

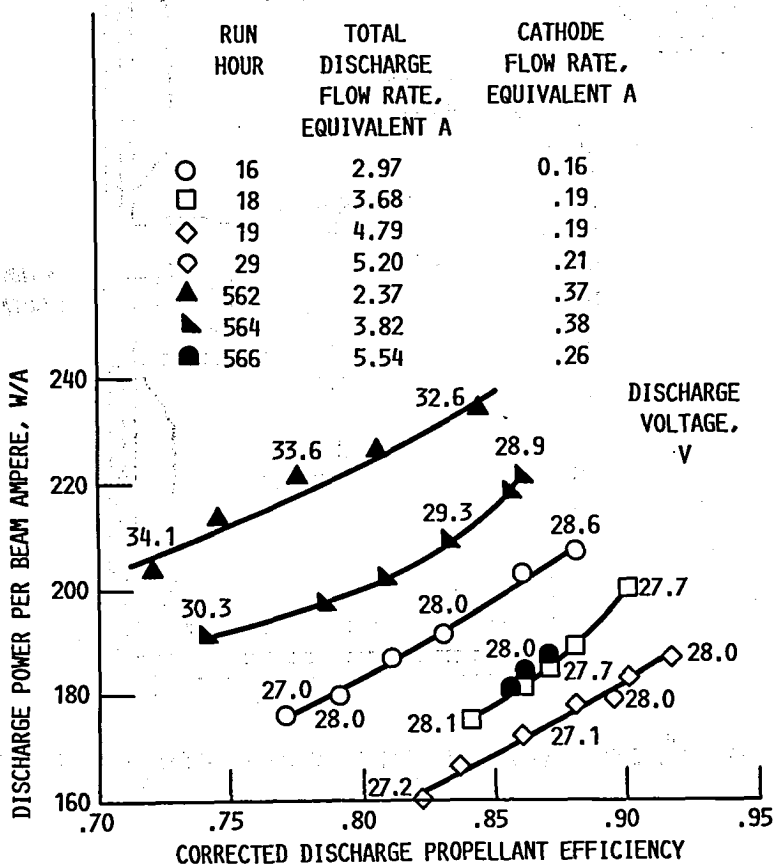

FIGURE 6. - DISCHARGE CHAMBER PERFORMANCE AS FUNCTIONS OF THE DISCHARGE FLOW RATE AND TEST TIME.

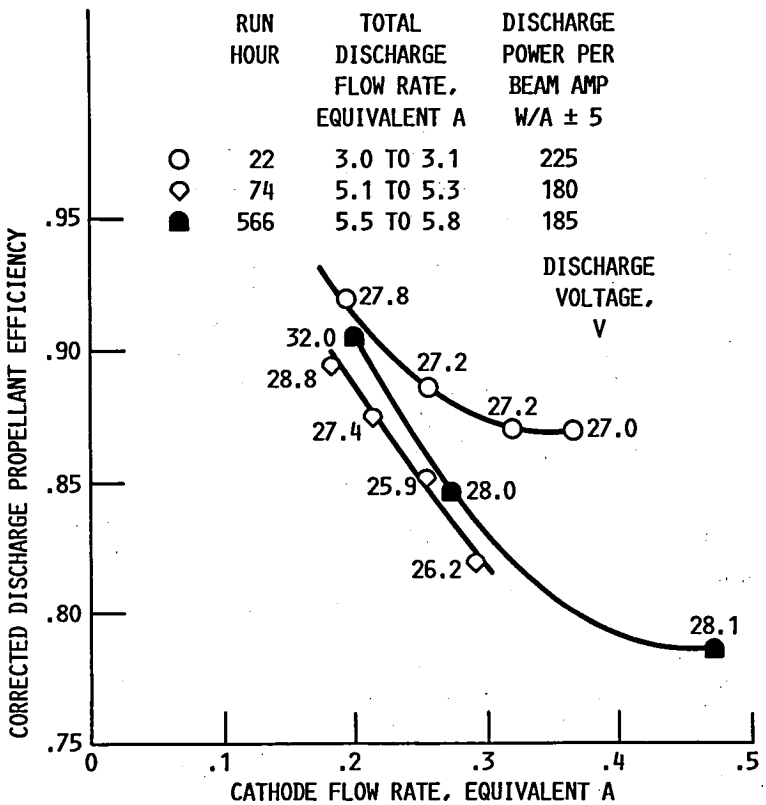

FIGURE 7. - PROPELLANT EFFICIENCY AS A FUNCTION OF CATHODE FLOW RATE; CONSTANT DISCHARGE CURRENT, MAIN FLOW RATE.

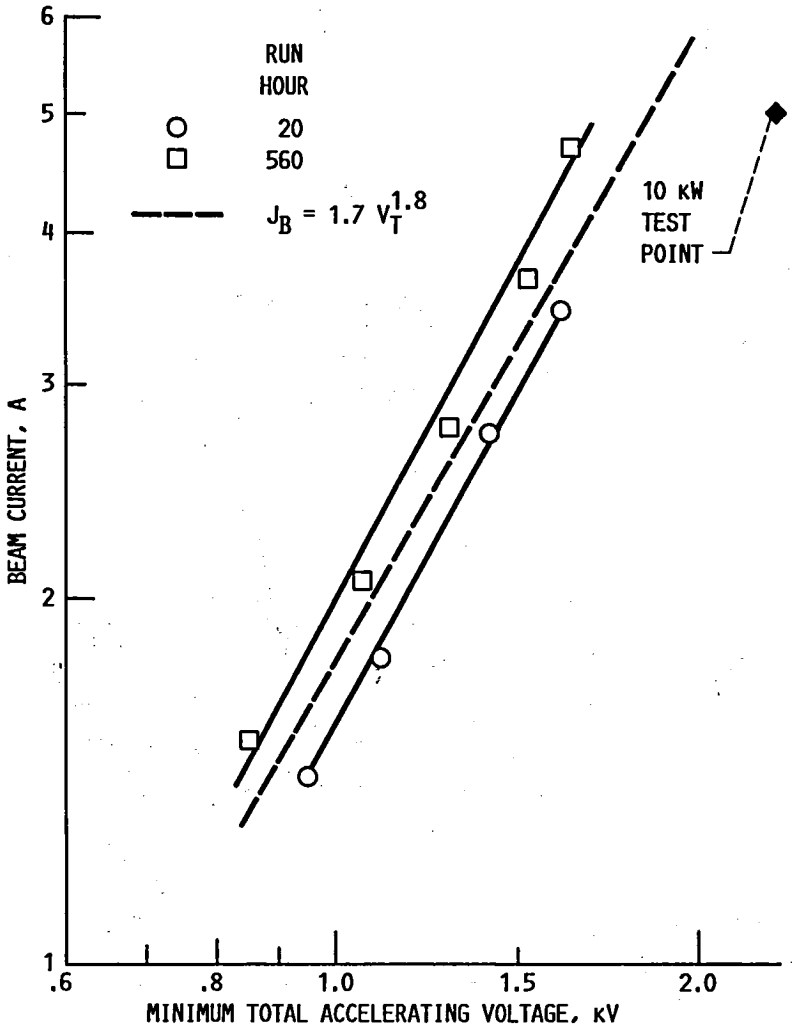

FIGURE 8. - CURRENT CARRYING CAPABILITY OF ION EXTRACTION SYSTEM.

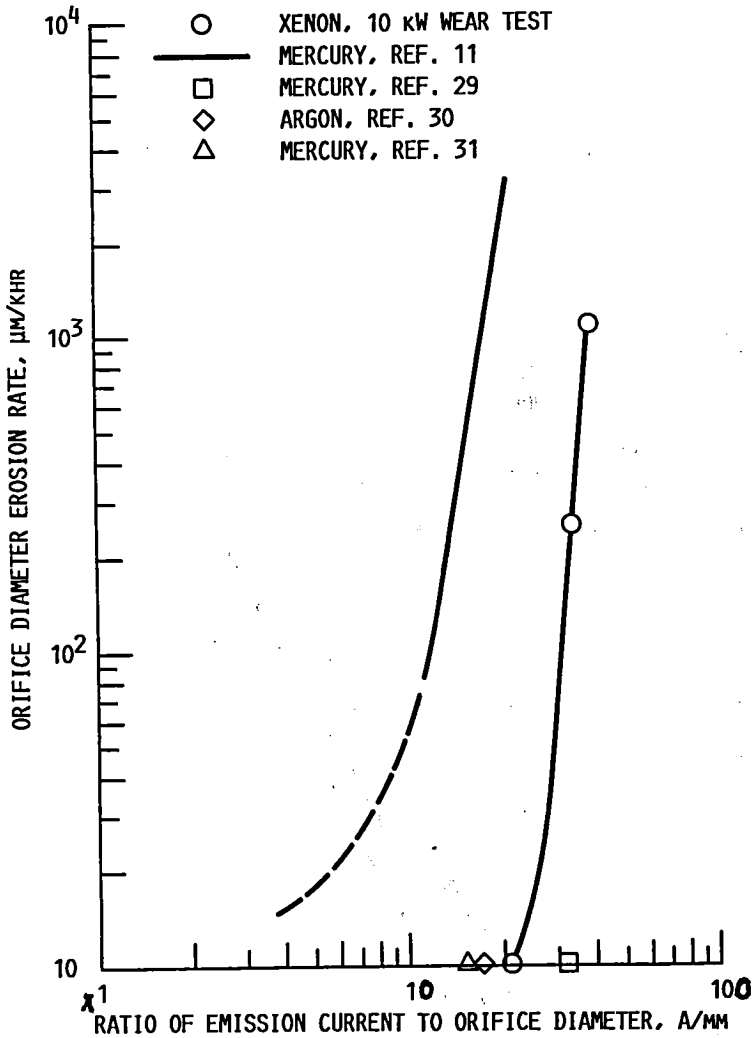

FIGURE 9. - CATHODE ORIFICE DIAMETER EROSION RATE AS A FUNCTION OF THE RATIO OF EMISSION CURRENT TO ORIFICE DIAMETER.

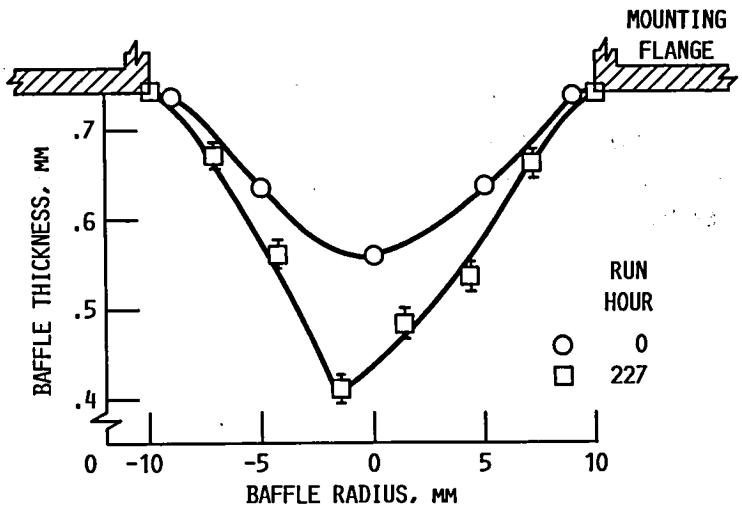

FIGURE 10. - IRON UPSTREAM BAFFLE THICKNESS AS A FUNCTION OF BAFFLE RADIUS AND TEST TIME.

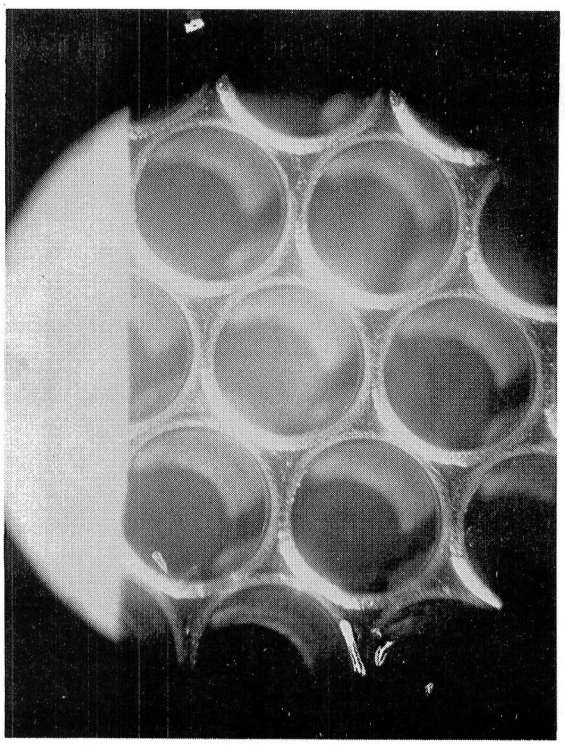

(a) UPSTREAM SIDE, BEFORE TEST.

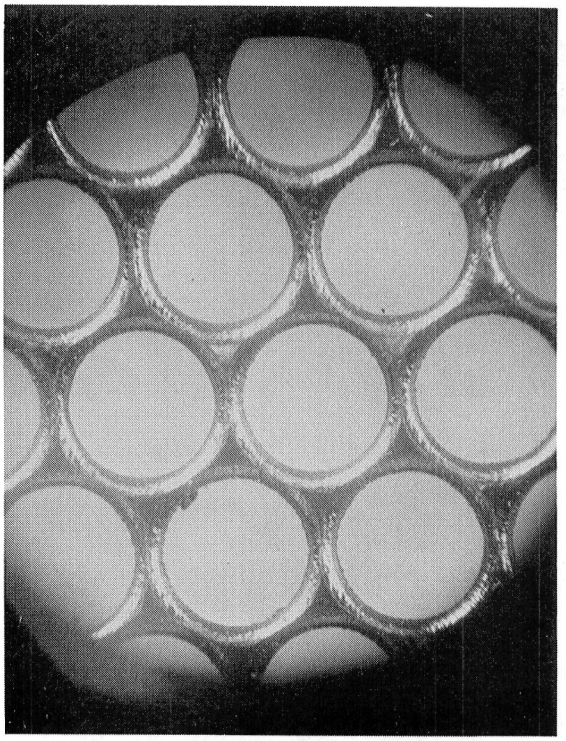

(b) UPSTREAM SIDE, AFTER TEST.

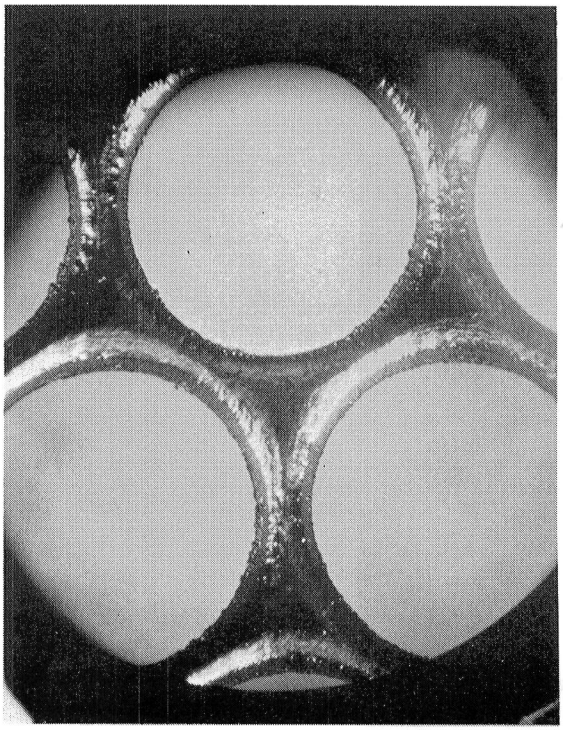

(c) UPSTREAM SIDE, AFTER TEST.

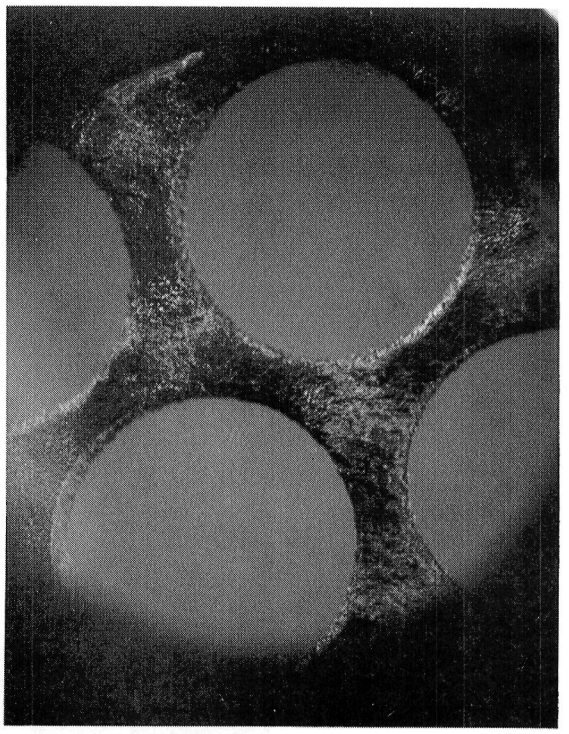

(d) DOWNSTREAM SIDE, AFTER TEST.

FIGURE 11. - SCREEN GRID.

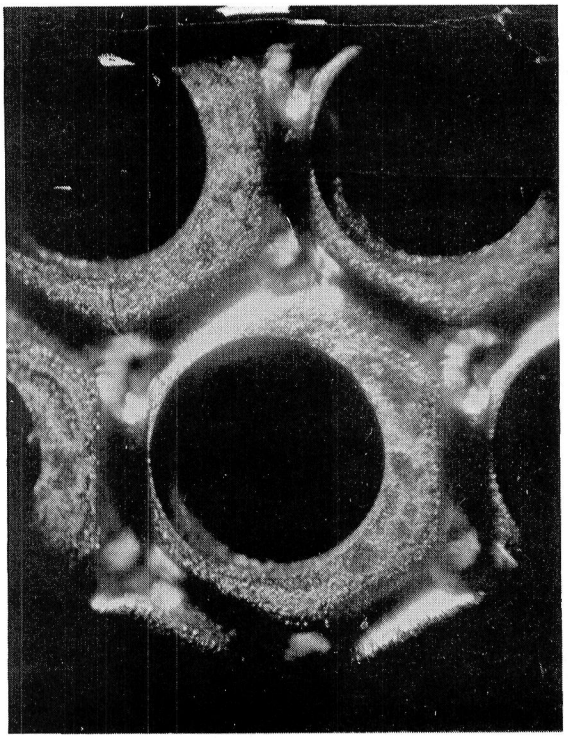

(a) DOWNSTREAM SIDE, BEFORE TEST.

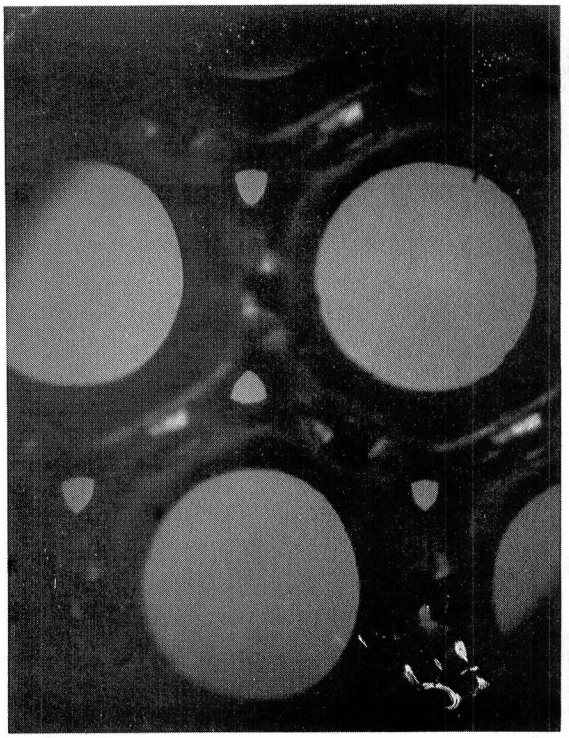

(b) DOWNSTREAM SIDE, AFTER TEST.

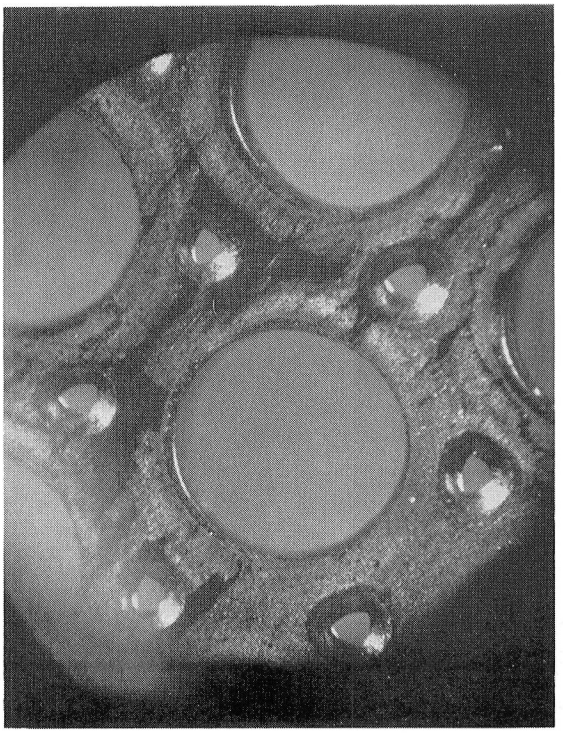

(c) UPSTREAM SIDE, AFTER TEST.

FIGURE 12. - ACCELERATOR GRID.

NASA
National Aeronautics and Space Administration

Report Documentation Page

1. Report No.	2. Government Accession No.	3. Recipient's Catalog No.
NASA TM-100954 AIAA-88-2912		

4. Title and Subtitle

Internal Erosion Rates of a 10-kW Xenon Ion Thruster

5. Report Date

6. Performing Organization Code

7. Author(s)

Vincent K. Rawlin

8. Performing Organization Report No.

E-4228

10. Work Unit No.

506-42-31

9. Performing Organization Name and Address

National Aeronautics and Space Administration
Lewis Research Center
Cleveland, Ohio 44135-3191

11. Contract or Grant No.

13. Type of Report and Period Covered

Technical Memorandum

12. Sponsoring Agency Name and Address

National Aeronautics and Space Administration
Washington, D.C. 20546-0001

14. Sponsoring Agency Code

15. Supplementary Notes

Prepared for the 24th Joint Propulsion Conference cosponsored by the AIAA, ASME, SAE, and ASEE, Boston, Massachusetts, July 11-13, 1988.

16. Abstract

A 30 cm diameter divergent magnetic field ion thruster, developed for mercury operation at 2.7 kW, was modified and operated with xenon propellant at a power level of 10 kW for 567 hr to evaluate thruster performance and lifetime. The major differences between this thruster and its baseline configuration were elimination of the three mercury vaporizers, use of a main discharge cathode with a larger orifice, reduction in discharge baffle diameter, and use of an ion accelerating system with larger accelerator grid holes. At a xenon ion beam current of 5 A the engine produced a thrust of 0.33 N at a specific impulse of 4220 sec and an efficiency of 68 percent. There was no measurable screen grid erosion. However, grid thickness measurement uncertainties, combined with estimates of the effects of reactive residual facility background gases gave a minimum screen grid lifetime of 7000 hr. Discharge cathode orifice erosion rates were measured with three different cathodes with different initial orifice diameters. As the initial orifice diameter was increased from that of the baseline value, the erosion rate decreased to near zero. Three potential problems were identified during the wear test. First, the upstream side of the discharge baffle eroded at an unacceptable rate, nearly two orders of magnitude greater than that of the baseline mercury thruster. Second, two of the main cathode tubes experienced oxidation, deformation, and failure after 227 and 243 hr of thruster operation. These failures are believed to be related to the cathode starting technique. Third, the accelerator grid impingement current was more than an order of magnitude higher than that of the baseline mercury thruster, implying a greater erosion rate. The impingement current increase is primarily due to a greater charge exchange ion current resulting from the higher beam current; operation at a higher neutral atom loss rate and; to a lesser extent, the higher facility pressure. The charge exchange ion erosion was not quantified in this test. There were no measurable changes in the accelerator grid thickness or the accelerator grid hole diameters.

17. Key Words (Suggested by Author(s))

Xenon
Ion thruster
Primary space propulsion

18. Distribution Statement

Unclassified - Unlimited
Subject Category 20

19. Security Classif. (of this report)	20. Security Classif. (of this page)	21. No of pages	22. Price*
Unclassified	Unclassified	30	A03

NASA FORM 1626 OCT 86

*For sale by the National Technical Information Service, Springfield, Virginia 22161

National Aeronautics and
Space Administration

Lewis Research Center
Cleveland, Ohio 44135

FOURTH CLASS MAIL

ADDRESS CORRECTION REQUESTED

Official Business
Penalty for Private Use $300

Postage and Fees Paid
National Aeronautics and
Space Administration
NASA-451